Executive summary

The main highlights of DeMStack can be summarized into three entities which refer to:

1. the manufacturing of robust MEAs with low Pt loading.
2. the mathematical modeling which assisted the efficient design of the bipolar plates and stack and can be used as a diagnostic tool for the quantitative understanding of the MEA processes
3. the design and manufacturing of the fuel cell stack integrated with a fuel processor.

New materials and MEAs

The understanding of the functional operation and degradation mechanisms of the fuel cell has advanced our knowledge and led to targeted modifications into a reliable product. New materials (Polymer Electrolyte Membranes) and electrocatalysts (Pt/(ox-MWCNTs)-Py) were developed and successful scaled up and resulted in more efficient performance. The MEAs are more robust in terms of their thermal stability and more efficient in Pt utilization in the catalytic layers both at the anode and the cathode. Lower Pt loadings (reduced by a factor of two) are achieved through the optimization of the electrocatalyst structure. The new Pt catalyst supported on pyridine modified CNTs exhibits significantly higher tolerance to reformate mixtures with increased water content even up to 30kPa and 2kPa CO. Beyond the already mentioned decrease in Pt loading, this improved performance can allow for the simplification of the BoP due to the decrease of the size of the water condenser at the fuel processor's exit.

Mathematical modeling and parameters determination

The mathematical modeling has being developed on two levels. The first is to be used as a diagnostic tool in order to simulate experimental data based on potentiostatic and especially potentiodynamic experimental data, aiming to the extraction and determination of the various parameters that are related to the efficient operation of the MEA. Under this approach special attention is given on the simulation of AC impedance spectra and the detailed simulation of the electrochemical processes within the catalytic layer. The second level refers to the holistic simulation of the fuel cell stack in order to optimize the design of the bipolar plates in terms of flow distribution and mass transfer, as well as heat transfer and temperature distribution along the MEA.

Stack and fuel processor design and construction

DeMStack optimized, designed, manufactured and tested under variable conditions a highly efficient, low-cost 1 kW HT PEMFC stack prototype constructed from optimized components. More specifically, two separate stack designs were considered. The one is based on metallic bipolar plates (Prototech) with internal cooling and the other on graphitic bipolar plates (Advent, FORTH) with external cooling. Both incorporating a liquid cooling system adjusted to the design. Different designs for the bipolar plates and materials were explored. After the design of the stacks and the selection of the component materials, the two stacks were constructed and pre-tested. In parallel, the system design including the fuel processor, the PCB control circuit with integrated microprocessor and other peripherals were completed. The fuel processor operating on natural gas or LPG was successfully integrated with the graphitic stack. Subsequently, the robustness of the system, the simplicity of the BoP, the operational stability and the user friendly operation of the integrated system into a commercially reliable product was demonstrated.

Summary description of the project context and the main objectives

High Temperature Polymer Electrolyte Membrane Fuel Cells having certain advantages over the state-of-the-art low temperature fuel cells constitute a key research issue aiming at higher efficiencies, cost reduction and compactness. One of the most important issues for the market penetration of fuel cells is their reliability and long term stable operation. More specifically, the activities of the DeMStack project were on the stack optimization and construction based on the high temperature MEA technology of ADVENT S.A. and its testing in combination with a fuel processor.

DeMStack goal was to enhance the lifetime and reduce the cost of the overall HT PEMFC technology. The strategy aimed at improvements based on degradation studies and materials development carried out in previous (FCH JU DEMMEA 245156) and ongoing projects that would lead to a reliable cost-effective product that fulfils all prerequisites for relevant field uses. These improvements cope with degradation issues related to catalyst utilization, reformate feed contaminants, uniform diffusivity and distribution of reacting gases in the catalytic layer and startup-stop and thermal cycles.

In this respect, DeMStack aimed to design, manufacture and test under variable conditions a highly efficient, low-cost HT PEMFC 1 kW stack constructed from optimized components, manufacture a fuel processor operating on natural gas or LPG and combine the two sub-systems. The consortium followed two different approaches/stack designs. One design was based on existing technology using graphitic plates and external cooling, a low risk task with great scientific and practical impact. The other used metallic plates with internal cooling, which is more challenging, but has the potential to broaden the applications and address needs of the market.

The project addressed the following scientific and technological issues regarding the successful implementation of a HT PEMFC Stack into a sustainable hydrogen society:

- H_3PO_4 doped High Temperature Membrane Electrode Assemblies (HT-MEA), being able to operate on a long term basis at temperatures above 180^{o}C.

The advanced state of the art MEAs were based on H_3PO_4-imbibed cross linked aromatic polyethers bearing pyridine units which can act as basic polar groups and interact through an acid base reaction with the acid. These MEAs are being manufactured by Advent and have been successfully developed within previous FCH JU projects. The objective within DeMStack was to refine the chemical structure in order to optimize the properties and scale up their synthesis.

- Catalytic layers for the HOR and ORR of alternative architectures. The goal was to results in improved features related to lower Pt loads >50%, full Pt surface electrochemical utilization at the electrode/electrolyte interface approaching 90% and increased stability. Two directions were followed. A catalytic layer based on pyridine modified carbon nanotubes for the HOR (under reformate) of minimal Pt loading and Pt supported on metal oxide modified CNTs for the ORR aiming at increased activity and stability.
- Bipolar plates of novel design which can promote the operating performance of the MEA. This task was assisted through targeted modeling and experimental methodologies. The flow field design of the stack's bipolar plates has to ensure the uniform distribution of the reacting gases along the catalyst layer and the electrochemical interface.
- Simplified design and manufacturing of the cell and stack configurations. Moreover, a very important part of developing the stack is the choice of materials for the sealing, bipolar plates and protective coatings able to withstand the harsh conditions of HT operation.
- Increased efficiency, robustness, durability and cost decrease in HT PEMFCs.
- Construction of a fuel processor working on LPG or Natural gas, specially designed to meet the specifications set for the operation of the fuel cell (e.g. hydrogen flow-rate, inlet pressure, hydrogen purity) and able to follow different operating scenarios (e.g. running in reduced capacity, different produced hydrogen purity, and multi-cycles operation etc).

o A “ready to use” integrated “fuel processor/fuel cell stack” system that can ensure the smooth and effective operation of each sub-system and operate with high electrical and overall CHP efficiencies.

The “product” of the DeMStack project is the integrated system prototype with the following operating features:

Fuel cell Stack:

(i) Fuel Cell Stack Power output of 1 kW (small scale-domestic category) operating on reformates with electrical efficiency exceeding 40% and operating temperature 180^{o}C.

(ii) Operation over a wide range of reformates, (H2=50-100%, CO = 0-4%, steam = 0-30%).

(iii) Overall cost reduction by a factor of 2 resulting by the significant reduction of the MEA’s cost due to the lower Pt loading and the cheaper membranes.

Integrated system:

(i) Power output 0.9 kW with electrical efficiency >38%.

(ii) Operation under steady state and dynamic conditions within a wide range of power output (0.5-0.9 kW).

Description of the main S & T results/foregrounds

1. Electrolytes (ADVENT, FORTH)

Advent's role on the project was focused on two areas. The first was the development, optimization and scaling up of polymer electrolytes and MEAs able to work up to 210°C under CHP conditions. The second, was the optimization of stack components and construction of a HT PEM fuel cell stack of 1 kW power output operating at 180°C on reformate gas, as will be described later on.

Regarding the first part of the work, the target was the large scale preparation of crosslinked and doped membranes and the manufacturing of the corresponding membrane electrode assemblies (MEAs). Factors such as final polymeric structure, monomer ratio, polycondensation conditions (solvents, temperature) and film processing have been investigated thoroughly. Many attempts took place, all of them based on aromatic polyethers bearing pyridine groups and side chain functional groups with cross linking ability as shown in the general structure of Scheme 1 below:

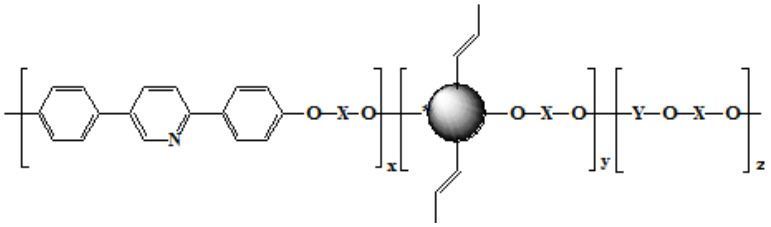

Scheme 1: General chemical structure of cross-linkable Demstack polymer electrolyte

After tuning the polymer composition (x,y,z) and crosslinking degree, the polymer synthesis was successfully scaled up. MEAs of 25 cm^2 were tested with a variety of feed gases and under continuous operation conditions showing high stability over time. After selecting the best candidate-which showed higher performance and a degradation rate of 5 μV/hr at 210°C with H_2/Air- large quantities of 360 g of the polymer and surface area of 0.2 m^2 for the films were prepared. This amount of ~400 g proved the scalability of the polymer synthesis process and was more than sufficient for the MEAs needed for the two HT PEMFC stacks of the project since this quantity would correspond to stacks of 4.3 kW of power.

2. Electrocatalysts (FORTH, CIDETEC)

A. Pt catalysts supported on modified carbon nanotubes (FORTH)

In a previous project, DEMMEA 245156, an approach toward the development of Pt-based electrocatalytic layers with increased catalyst utilization for use in high temperature PEMFCs was achieved and reported [Applied Catalysis B: Environmental 106, 2011, 379]. More specifically, multi-wall carbon nanotubes (MWCNTs) were used as the support and were chemically modified to result in a uniform distribution of covalently attached polar pyridine groups. Pyridine groups are able to interact with phosphoric acid achieving increased contact of the active phase (Pt) with the proton conductor and thus the extension of the electrochemical interface and the increase of the catalyst utilization. Within the framework of DeMStack, the reactions for both the functionalization of nanotubes (no-solvent functionalization method) and the deposition of Pt (polyol method) were optimized and scaled up. A representative TEM image of the obtained catalyst is shown in Figure 1.

Moreover, its performance under reformate conditions and optimization of electrodes construction parameters (amount of Pt and phosphoric acid) took place. A short summary is given below. The highest performance of a fuel cell is achieved when pure hydrogen is employed as fuel, however the most common and cost effective route for production of hydrogen is through steam reforming of hydrocarbons and water gas shift reactions for the production of the so called reformate gas. These methods produce carbon monoxide as a byproduct, the concentration of which has to be dramatically

reduced in order to be suitable for PEM fuel cell applications. Although high temperature PEM fuel cells are highly tolerant towards CO poisoning, under certain reformate conditions the performance of the anode is severely affected. This negative effect appears in relation to the structure of the active electrochemical interface, as this is specified by the amount of PA on the electrode, when high partial pressure of water is present in the reformate gas (A.Orfanidi et al, J Appl Electrochem 43 (2013) 1101–1116 & M. Georgmezi et al, J Power Sources 285 (2015) 499-509). Within DeMStack the work of FORTH focused on the creation of an electrocatalytic layer that can operate in a HT PEM fuel cell using reformate gas consisting of high CO and steam mole fraction without sacrificing its performance. The reason is that the ultimate goal of the DeMStack project is coupling the FC stack with a reformer.

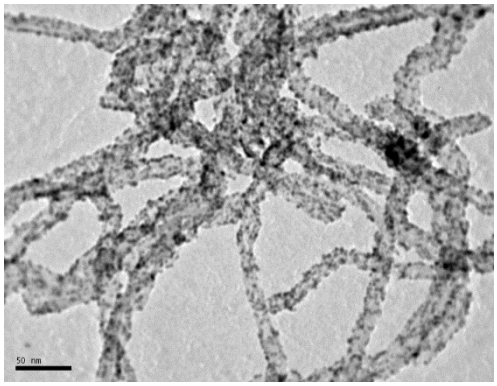

Figure 1. TEM image of 30% Pt/(ox.MWCNT)-Py.

In this respect, the selected electrocatalyst 30 wt% Pt/(ox.MWCNT)-Py was thoroughly evaluated and compared to Pt/ox.MWCNT, as well as the commercial 30% Pt/C (Tanaka). A parametric analysis took place, where the effect of each component that participates in the reformate gas composition and the behavior of the different catalyst substrates were studied. The performance degradation mechanisms were identified. The interaction of both CO and water with the catalyst surface, as well as the influence of PA and its distribution in the catalyst layer, appear to be the key in the optimization of the HT PEM system working under these harsh conditions.

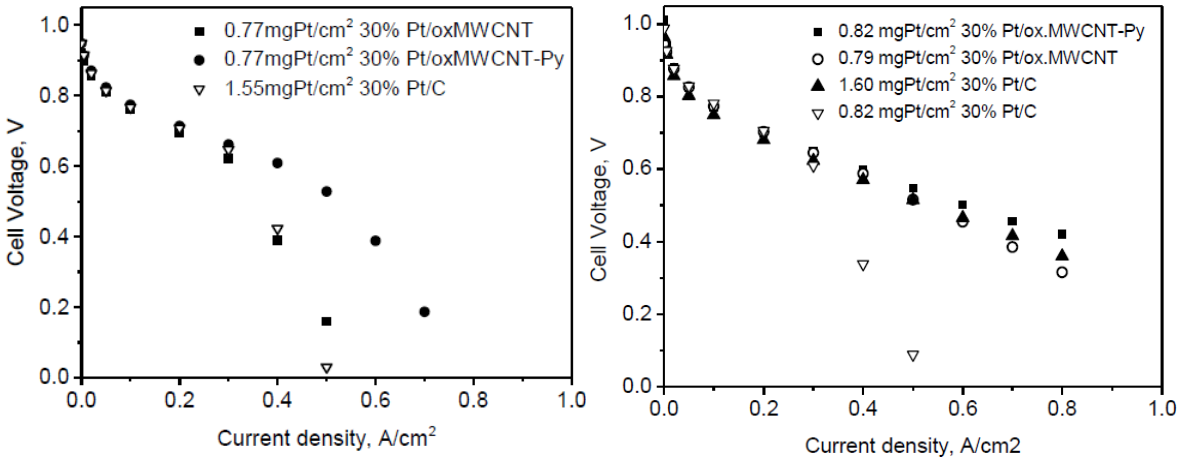

Figure 2. The effect of the catalyst substrate on the anode's performance at 180°C under synthetic reformate gas consisting of 50.7 kPa H_2, 2 kPa CO and 33.5 kPa H_2O balanced with Ar. The polarization curves were obtained using a stoichiometry of λ_{H2}=1.2 and λ_{O2}=2, pure O_2 was used at the cathode. The PA loading at the anodic electrode was (a) 2 gPA/gPt and (b) 0.5 gPA/gPt.

An example is presented in Figure 2a, which shows the effect of the catalyst substrate on the fuel cell's performance when synthetic reformate was fed at the anode. In these MEAs, the anodic

electrode was sprayed with 2 gPA/gPt. At low current densities there are adequate Pt sites free for the H_2 electro-oxidation reaction, as the poisoning effect is negligible, and therefore the performance of the fuel cell is not severely affected. As the current density increases, the HOR is being constrained by the remaining free Pt sites due to blockage of the Pt surface by poisoning adsorbents. At current densities higher than 0.4 A/cm^2, there is a shortage of available free Pt active sites, reaching limiting current. The MEA employing the commercial catalyst 30% Pt/C (1.55 mgPt/cm^2), suffered a significant voltage loss. Similar behavior was observed for the MEA employing 30% Pt/ox.MWCNT, reaching the same short circuit current, but having half the Pt loading in the catalytic layer (0.77 mgPt/cm^2). A substantial improvement of the cell's performance was observed when the 30% Pt/oxMWNT-Py electrocatalyst was used under the same conditions. The pyridine modified MWCNT based electrocatalyst reached a short circuit current value of approximately 0.7 A/cm^2 having a noble metal loading equal to 0.77 mgPt/cm^2. The amount of PA on the electrodes plays a significant role in the formation of the electrochemical interface. In Figure 2b the MEAs employ 0.5 gPA/gPt at the anode. The MWCNT based electrocatalysts exhibited high endurance and performance. In the case of 30% Pt/C we had to incorporate high loadings in order to achieve similar performance.

The anode's performance loss under harsh reformate conditions can be attributed to the restructuring of the electrochemical interface, as a result of the synergistic effect of the PA amount and the water solvation in the distributed PA within the catalytic layer. As PA is being sprayed on the catalyst layer, uniform distribution is not guaranteed. The distribution of PA within the catalytic layer depends on the hydrophobicity of the catalyst, the pore size distribution and the porosity of the catalytic layer. Ideally, the optimum PA distribution would be the formation of a thin film over the Pt surface homogeneously distributed in the catalytic layer. The concentration of PA depends on the reactant's gas humidification (partial pressure of water) and the operation temperature. When phosphoric acid is exposed to water vapor at elevated temperature an equilibrium is established. It can be assumed that upon water solvation the PA areas swell. This may cause ganglia formation inside the pores' channels, blockage of the pores and the disruption of the continuous distribution of the PA, thus resulting into the shrinkage of the electrochemical interface as well as gas transport limitations.

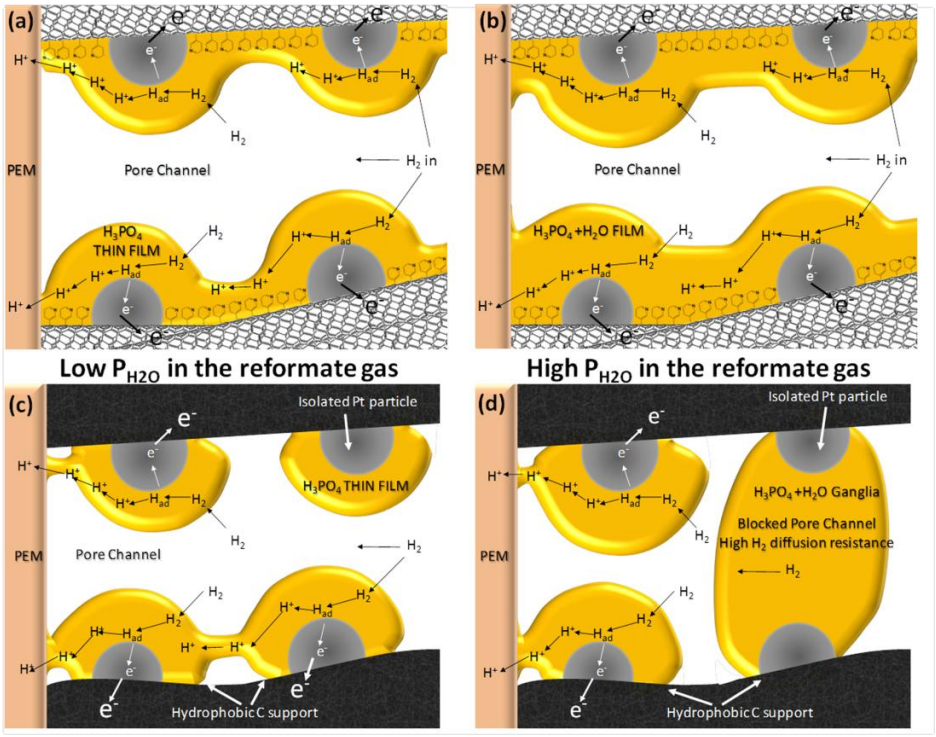

Figure 3. Schematic representation of the electrochemical interface under low (a and c) and high (b and d) partial pressure of steam for Pt/(ox.MWCNT)-Py (a and b) and Pt/C (a and d) catalysts.

This is illustrated in Figure 3 and is believed to be taking place in the case of Pt/C. At low partial pressure of water in the reformate mixture, the equilibrium concentration of solvated water in PA is lower and the PA film does not swell to such degree to result in the ganglia formation and the blockage of the pore channels or the disruption of the ionic pathway, thus inducing small changes to the anode's performance.

The 30 wt% Pt/oxMWCNT-Py electrocatalyst proved to be the ideal candidate for operation under harsh reformate conditions. The interaction of pyridine groups with phosphoric acid not only promotes its uniform distribution on the CL but also stabilizes the electrochemical interface under high partial pressure of water. Additionally, the use of pyridine functionalized MWCNT based electrocatalyst gives the opportunity of lowering the Pt loading in the electrodes without sacrificing the overall cell's performance under reformate conditions, thus reducing the MEA production cost.

B. Pt catalysts supported on metal oxide coated CNTs (CIDETEC)

The goal was related to the development of electrocatalysts with improved stability and activity. The particle stabilization and activity of Pt on the CNT supports can be improved by the dispersion of transition metal oxide layers and/or particles on the surface modified CNTs. Metal oxides will serve as strong anchoring centers, due to the abundance of surface oxygen groups, while the stronger adhesion of the metal clusters on the metal oxide surface is expected to affect the catalyst activity and inhibit sintering. In this context, the objective was to prepare Pt supported on metal oxide modified CNTs, and to test their electrochemical activity towards the oxygen reduction reaction (ORR) for their application as cathode in HT PEMFC.

First of all, a procedure to functionalize the surface of commercial multiwall carbon nanotubes, MWCNT, (diam.: 15-35 nm, length $\geq$ 10 μm, surface area: 200-250 m^2 g^{-1}) was developed. This procedure was based on a chemical oxidation treatment, which allowed obtaining a high degree of functionalization (ox.MWCNT). In addition, it was easily scaling-up. The temperature programmed desorption (TPD) analysis of functionalized MWCNT revealed that the main surface group was –COOH (13 % mol.). Thermogravimetric analysis (TGA) was also applied to study the stability of functionalized CNTs. As mentioned above, the presence of pyridine groups in the anode catalyst support improved the catalyst utilization and stability in the anode of a HT PEMFC, fed with reformate. Considering this, we also studied the effect of pyridine groups in the cathode catalyst support on the HT PEMFC performance.

Metal oxides were dispersed onto the functionalized carbon nanotubes ox.MWCNT or ox.MWCNT-Py, provided by FORTH, using a metal precursor in aqueous solution, by means of different chemical approaches. This lead to catalyst support, whose composition was ox.MWCNT-(Py):X (X= CeO_2, CoOx, TiO_2) 80:20 wt. %, and crystallite sizes from 3.6 to 7.7 nm.

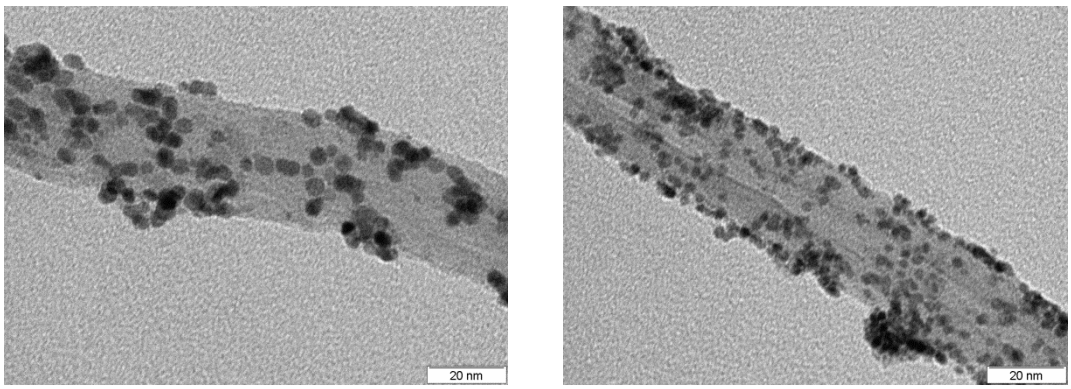

Figure 4. Selected TEM images of Pt/ox.MWCNT-CeO_2 (left) Pt/CNT-Py-CeO_2 catalysts (right).

Thereafter, platinum supported catalysts (Pt 30 wt. % nominal) were synthesized by the *polyol method*, using the functionalized ox.MWCNT-(Py)-X (X= CeO_2, CoOx, TiO_2) supports. Pt/ox.MWCNT-X (X= CeO_2, CoOx, TiO_2) catalysts showed a crystallite size approximately of 3 nm, while for the Pt/ox.MWCNT-Py-X (X= CeO_2, TiO_2) catalysts it was around 2 nm. Figure 4 shows selected TEM images of catalysts Pt/ox.MWCNT-CeO_2 and Pt/ox.MWCNT-Py-CeO_2.

It seemed that the presence CeO_2 and pyridine groups favoured a further anchoring and dispersion of Pt nanoparticles. In addition, element distribution maps (not shown) allow concluding that Pt and Ce or Ti was homogeneously distributed around carbon nanotubes.

On the other hand, the activity of the synthesized catalysts towards the oxygen reduction reaction (ORR) was investigated in rotating disk electrode (RDE) and modified gas diffusion electrode (GDE) setups, using H_3PO_4 (conc.) as electrolyte at 20 and 160 °C. The latter configuration allowed feed the electrode with air, a similar situation than that found in a real HT PEMFC. Moreover, the potential resistance of catalysts against H_3PO_4 poisoning was evaluated comparing the electrochemically active surface areas (ECSAs), determined from the $H_{ads.}/H_{des.}$ region in cyclic voltammograms in $HClO_4$ and H_3PO_4. The results obtained showed that catalysts Pt/ox.MWCNT-CeO_2 and Pt/ox.MWCNT-TiO_2 were less prone to poison in H_3PO_4 solutions. The determination of $E_{1/2}$ potentials confirmed that CeO_2 and TiO_2 inhibit the phosphate poisoning effect on the ORR.

The main achievements of this of task are as follows:

- ox.MWCNT-(Py)-X (X = CeO_2, CoOx, TiO_2) supports were synthesized by a simple chemical method at nanometric scale.
- Pt/ox.MWCNT-(Py)-X (X= CeO_2, CoOx, TiO_2) were successfully manufactured with good dispersion. These catalysts showed activity towards ORR, in particular, those which contained CeO_2 and TiO_2.
- In general, it seemed that Pt catalysts supported on modified ox.MWCNT-X (X = CeO_2, TiO_2) were less prone to adsorb species coming from the dissociation of H_3PO_4, than Pt on ox.MWCNT.

Moreover, in order to define and tune the optimum parameters that constituted a good, efficient and robust MEA based on the catalysts Pt/ox.MWCNT-(Py)-X (X= CeO_2, TiO_2), the following MEAs were manufactured:

Pt/C (30 wt. %) (1.0 $mg_{Pt}cm^{-2}$)|TPS®|Pt/ox.MWCNT (1.0 $mg_{Pt}cm^{-2}$)
Pt/C (30 wt. %) (1.0 $mg_{Pt}cm^{-2}$)|TPS®|Pt/ox.MWCNT-X (X= CeO_2, TiO_2) (1.0 $mg_{Pt}cm^{-2}$)
Pt/C (30 wt. %) (1.0 $mg_{Pt}cm^{-2}$)|TPS®|Pt/ox.MWCNT-Py (1.0 $mg_{Pt}cm^{-2}$)
Pt/C (30 wt. %) (1.0 $mg_{Pt}cm^{-2}$)|TPS®|Pt/ox.MWCNT-Py-X (X= CeO_2, TiO_2) (1.0 $mg_{Pt}cm^{-2}$)

MEAs were tested in HT-PEMFC test bench at relevant experimental conditions, to gain knowledge useful for the HT PEMFC stack operable at and above 180 °C. After the break-in, a series of experimental techniques and conditions were used: IV plots at different temperatures (180, 160, and 140 °C), H_2 crossover measurement and CO stripping at 140 °C, as well as, BoL test at 0.2 A cm^{-2} and 180 °C for 168 or 336 h (1 or 2 weeks, respectively). Table 1 depicts the performance of MEAs before and after the BoL test.

According to the results, the use of CeO_2 in the catalyst support ox.MWCNT-CeO_2 increased the initial MEA performance compared to the ox.MWCNT support, but not the stability. However, the opposite was observed with using TiO_2 (ox.MWCNT-TiO_2): the MEA performance was lower compared to the ox.MWCNT support, but the stability was higher. It is worth to mention that the combination of metal oxides with pyridine groups present in ox.MWNCTs seemed to have a synergistic effect: the stability of the MEA containing Pt/ox.MWCNT-Py-CeO_2 and the performance of the MEA containing Pt/ox.MWCNT-Py-TiO_2 increased.

In conclusion, the results of the TPS® MEA characterization in HT PEMFC showed that the use of TiO_2 in the catalyst support ox.MWCNT seemed to increase the stability of cathodes in the MEA

environment. The presence of pyridine groups in the ox.MWCNT support provided an added value in terms of a performance increase.

Table 1. Comparison of MEA performance before and after BoL test at 180 °C.

MEA	OCV / V	*V* @ 0.2 A cm^{-2} (0 h) / V	*V* @ 0.2 A cm^{-2} (168 h) / V
Pt/ox.MWCNT	0.946	0.612	0.577
Pt/ox.MWCNT-CeO_2	0.944	0.650	0.559
Pt/ox.MWCNT-TiO_2	0.944	0.557	0.577*
Pt/ox.MWCNT-Py	0.910	0.605	0.607
Pt/ox.MWCNT-Py-CeO_2	0.900	0.594	0.604
Pt/ox.MWCNT-Py-TiO_2	0.925	0.606	0.600

*(0.559 V after 336 h)

3. Development of the rotating rod methodology for the kinetic study of Pt/C electrocatalysts in hot phosphoric acid (UCTP)

Here the attention was focused on development and validation of an electroanalytical method/tool for easy and effective HT PEM FC catalyst activity testing under HT PEM FC relevant conditions (120-200 °C, concentrated H_3PO_4). At the moment, such a method is not available due to limitations of commercially available rotating disc electrodes. The developed rotating rod electrode is based on glassy carbon rod on which bottom part a thin-film with tested catalyst is prepared. Glassy carbon was chosen as relatively innert and stable material with high overpotential for oxygen reduction/evolution. The rod electrode was first verified by comparing to commercial rotating disc electrode at room temperature using standard $Fe(CN)_6^{3-}/Fe(CN)_6^{4-}$ couple. The results showed that there is some difference between the limitting currents/apparent diffusion coefficients of $Fe(CN)_6^{4-}$, see Figure 5A. This effect was consequently confirmed by hydrodynamic model of the electrolyte in the cell developed in COMSOL Multiphysics. The model allowed to explain the difference between experimental results by increased normal velocity of the flow towards the electrode (and consequently to a lower thickness of Prandl layer) in the case of rotating rod. Finaly it was shown that the effect of different flow hydrodynamics can be simply accounted for by changing the value of the constant (0.62) in Levich/Koutecky-Levich equation. The constant seems to be slightly kinematic viscosity dependent. In the last stage, the activity of HISPEC 4000 catalyst towards oxygen reduction reaction under conditions relevant for HT PEM FC operating conditions (160 °C, concentrated H_3PO_4) was evaluated.

4. Study of electrochemical behaviour of selected phosphorus acids on Pt electrode (UCTP)

Attention was focused also on the investigation of the basic electrochemical properties and behavior of various phosphorus oxoacids was studied as these compounds can be potentially formed from H_3PO_4 during HT PEM FC operation. These compounds could potentially influence HT PEM FC behaviour and understanding of the related processes will be of primary importance in understanding HT PM FC operation. The attention was focused mainly on H_3PO_3 which is sufficiently thermally stable and can exist at HT PEM FC operating temperature. The results showed that electrochemical behaviour of H_3PO_3 on a Pt electrode is quite complex. Besides its anodic oxidation on the both metallic Pt and oxidised Pt surface taking place at overpotential of around 1 V, there is also its large tendency to strongly adsorb on the Pt surface. The adsorption extent in aqueous solutions increases together with temperature and at elevated temperature (< 50 °C) exceeds monolayer coverage suggesting acid condensation leading to a formation of di/trimeric oxoacid at the surface. Adsorption

was also found to depend on the supporting electrolyte anion and electrode potential. H_3PO_3 anodic oxidation on metallic Pt seems to be quite a complicated process involving adsorption of not only H_3PO_3 itself but also adsorption of (intermediate) products largely slowing down the oxidation rate. H_3PO_3 oxidation on oxidised Pt surface was shown to proceed via chemical reaction between Pt oxides and H_3PO_3. Aside of H_3PO_3 also H_3PO_2 and $H_4P_2O_6$ were studied. The former behaves very much like H_3PO_3 documenting large effect of molecular structure of these ecids on their properties. The later seems rather inert against anodic oxidation on metallic Pt as its anodic oxidation takes place very slowly on the preoxidised Pt surface only. The oxidation was shown to proceed via electron transfer.

5. Improving HT PEM FC performance (UCTP)

We have successfully developed procedure/method allowing to improve HT PEMFC performance without further increasing Pt loading or changing MEA/cell components or operating temperature. This is documented by the current density increase, e.g. 0.45-0.6 A cm^{-2} (@ 0.6 V) for the "boosted" MEA as compared to 0.25-0.3 A cm^{-2} for standard MEA (@ 0.6 V), as shown by U-I curves in Figure 5B. The "boosting" was shown to be stable over more than 800 h of MEA operation (longer times were not tested due to the time constrains) and is still under investigation.

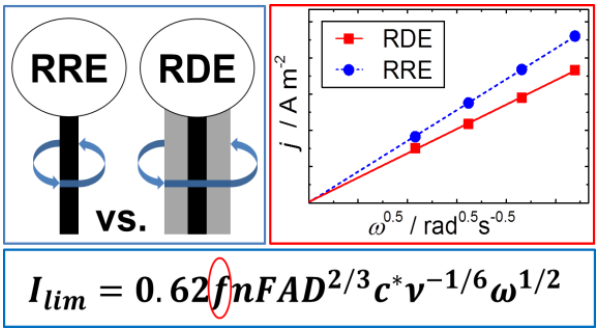

Figure 5A: Schematic comparison of rotating disc electrode (RDE) and rotating rod electrode (RRE) and corresponding limiting current densities described by the Levich equation given at the bottom. Correction factor f = 1 (for RDE) and f = 1.18 (for RRE).

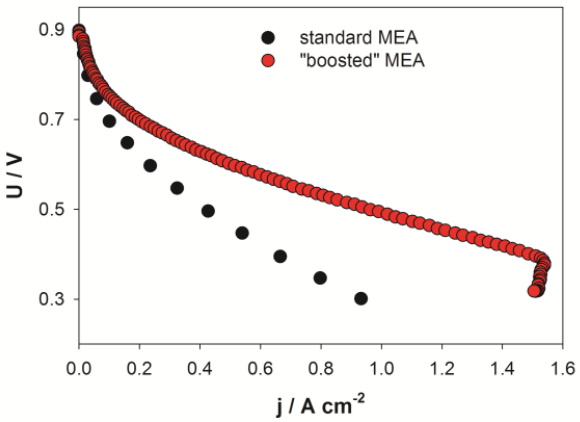

Figure 5B Examples of the load curves of the standard and "boosted" HT PEM FC (recorded after 200 h of constant voltage operation at 0.55 V. 160 °C, both electrodes loaded with 0.5 mg Pt cm^{-2} (40% Pt/C).

6. Catalyst degradation under well-defined conditions (UCTP)

The issue addressed here was the decrease of the electrochemically active surface area due to Pt nanoparticles growth during HT PEMFC operation. For these experiments, in-house prepared Gas Diffusion Electrodes incorporating commercial 40 wt% Pt on carbon black were used. In order to simplify the problem, all MEAs were operated at constant voltage for whole time of the experiments. This to some degree simulates keeping potential on the both electrodes constant. Consequently, the MEA's were disassembled and the crystallite size and particle size distribution on the individual MEA sides were determined using X-ray diffraction and small angle X-ray scattering, respectively. Analysis of the results showed that degradation in HT PEMFC is a complicated process even if the fuel cell is operated at constant voltage. A continuous and moderate growth of Pt crystallites and, correspondingly a decrease of Pt surface area, were observed at high fuel cell operating voltage (near open circuit conditions) for 2000 to 3000 hours. An Ostwald ripening was suggested to be most dominant Pt catalyst degradation mechanism. On the contrary, the Pt crystallites growth rate and

surface decrease rate were significantly faster at low operating voltages, though the experiments at these voltages were significantly shorter. The corresponding longer-term experiments at low cell voltage are currently being finalized. It is good to note that these experiments are extremely time-consuming. It seems that at lower cell voltage, the catalyst degradation is governed by different mechanisms, most probably by the crystallites sintering. At the moment, the rate of Pt catalyst degradation was approximated by empirical function and will be re-evaluated later once the few remaining experiments are finished, see Figure 6A. In the case of the anode, no obvious change of Pt crystallite size and surface area was observed within the error of the experimental procedure.

7. Characterization of mass transport properties of the catalyst layer

The objective of this work was the characterization of mass, heat and charge transport properties of the catalytic layer both experimentally and by mathematical simulation. First, using focused ion beam scanning electron microscopy (FIB-SEM) technique replicas of catalytic layer samples were obtained, Figure 6B.

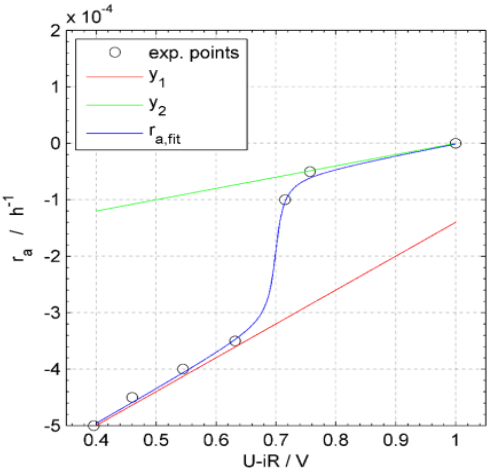

Figure 6A Dependence of rate of relative surface density of Pt decrease (at the cathode) in dependence on U-iR, dots - experimental data, y_1 and y_2 linear functions - auxiliary functions for fit, red line - the final fitted empirical function. r_a is defined as $r_a = d(a/a_0)/dt$ with a – active area per catalyst layer volume [m^2 m^{-3}], subscript 0 – in time t = 0.

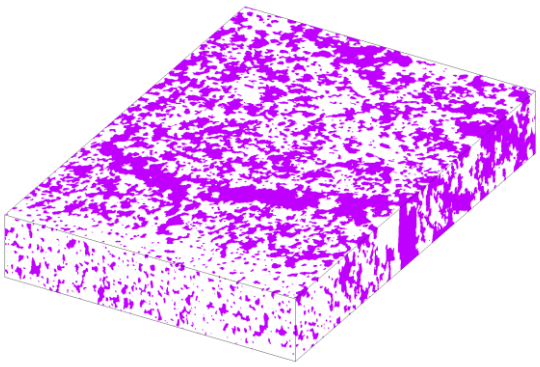

Figure 6B Replica of the fresh catalytic layer. The void and solid phases are magenta and white, respectively.

In the next step, permeation measurements of transport properties in a quasi-stationary permeation cell were performed. The evaluated data served for (a) quantification of viscous flow in the catalytic layer and (b) for verification of the replica computed from serial FIB-SEM tomography and validation of the mathematical simulator for effective transport parameters calculation. The simulations of ordinary self-diffusion in pore space taking place in the region of continuum and simulations of electrical conduction in the solid phase were successfully performed. Results are given in the form of main diagonal components of the geometric factor tensor and the electrical conductivity tensor. The effect of the statistically inhomogeneous and anisotropic microstructures of catalytic layer on effective transport properties of pore space is clearly seen. The gas permeation measurement through the catalytic layer, the development of the experimental set-up and mathematical processing of the experimental data is at the beginning. Therefore, a comparison of the experimental permeation data with the transport characteristics predicted using the random walk algorithm calculation in replica of the catalytic layer is not possible. Although the experimental set-up was developed for materials with

homogeneous and isotropic microstructure, the difference in the viscous flow parameters in the pure pellet and pellet with the catalytic layer is significant. From this point of view, this method looks promising for quantification of transport properties of catalytic layer. Our current aims are at (a) verification of this new approach on another pellet and (b) finding of differences between pristine and thermally treated catalytic layer. Next goal is to rearrange the mathematical processing of the experiments to obtain transport parameters of standalone catalytic layer without contribution of the alumina support. Final goal is comparison of the measured transport parameters with quantities from simulation of transport properties on catalytic layer replicas. This comparison will be a part of verification of catalytic layer microstructure.

8. Testing protocols (JRC-IET, FORTH, CIDETEC)

The development of robust AST protocols is required to assess the reliability of HT-PEM MEA when subjected to cycling and transient operating conditions. Standard test method such as polarisation (I-V) curve and electrochemical impedance spectroscopy (EIS) measurements are used to assess MEA performance prior to and upon cycling and transient operation conditions to determine whether the MEA is robust enough to withstand such harsh conditions.

Eventually it indicates whether the MEA tested will have an acceptable technical life being the main prerequisite for cost effective robust and reliable MEA components integrated into HT-PEM fuel cells operating at temperatures of 180˚C up to 200˚C. The developed AST protocols consist of three tests. The operating conditions including the test profiles are

- Test #1: targeting catalyst degradation by triangular voltage cycles between 0.70 V and 1.05 V of 16 seconds duration,
- Test #2: targeting electrolyte membrane degradation by rectangular voltage cycles between 0.50 V and 0.80 V of 16 seconds duration and dry air feed and
- Test #3: targeting anode degradation by rectangular voltage cycles between 0.50 V and 0.80 V of 16 seconds duration with simulated humidified reformed hydrogen gas as anode fuel feed.

The validation of the developed AST protocols by the obtained test result indicates the chosen operating conditions and test profiles are indeed suitable for their intended purpose.

For test #1, it was found that an increasing number of cycles (in sequence of 100 cycles, 500 cycles, 1,000 (1k) cycles, 5,000 (5k) cycles, 10,000 (10k) cycles and 14,500 (14.5k) cycles) the performance of HT-PEM MEA in terms of polarisation curves declines when compared to the beginning of test (BOT). More concrete, up to 10,000 triangular cycles the open circuit voltage (OCV) steadily reduces to about 600 mV while thereafter the OCV reduction is far more significant.

Apparently, the electrolyte membrane also degrades. Notably, the achievable maximum current density reduces significantly with increasing voltage cycles.

The conducted impedance measurement show that increasing voltage cycling leads to a reduction in the high frequency resistance and very significant increases in the polarisation resistance especially after 5,000 voltage cycles.

As regards test #2, it is evident from the observed performance that the MEA resist very well the imposed high number of rectangular voltage cycles. Only at the highest measured current density is some decline in the cell voltage most notable although the OCV is reduced by about 500 mV after 100,000 voltage cycles compared to BoT for test #2.

The high frequency resistance seems not to be affected much by voltage cycling and in contrast to the EIS measurements in test #1 the polarisation resistance appears not be altered by voltage cycling in test #2 which is confirmation that the MEA performed well.

It is noted that the OCV of the MEA are less affected compared to MEA subject to test #2.

The lower performance of the MEA under the conditions of test #3 compared to those of test #2 is attributable to the presence of water and CO and hence a lesser amount hydrogen in the fuel feed.

In test #3, the EIS measurements show that the high frequency resistance is of similar range to the ones obtained in performing test #2. But compared to this test, the polarisation resistance of the MEA subjected to the conditions of test #3 increased with increasing number of voltage cycles.

Overall it can be stated that the validation of the developed AST protocols by the obtained test result indicates the chosen operating conditions and test profiles are indeed suitable for their intended purpose.

Furthermore, the developed protocols may in agreement with the consortium serve as seeding documents in case the harmonisation efforts currently ongoing at JTI level for LT-PEM single cells targeting automotive and stationary applications are extended to HT-PEM MEA applications.

Finally, post-mortem analysis of aged MEAs at JRC-IET facilities were carried out by Cidetec, by means of TEM observations to determine the evolution of the nanoparticles and their support in different regions of the MEA (H_2 and O_2 inlet and outlet) tested in HT PEMFC. Cathode catalyst samples were taken from the cathode inlet and outlet of MEAs, respectively, by peeling-off the cathode from the membrane.

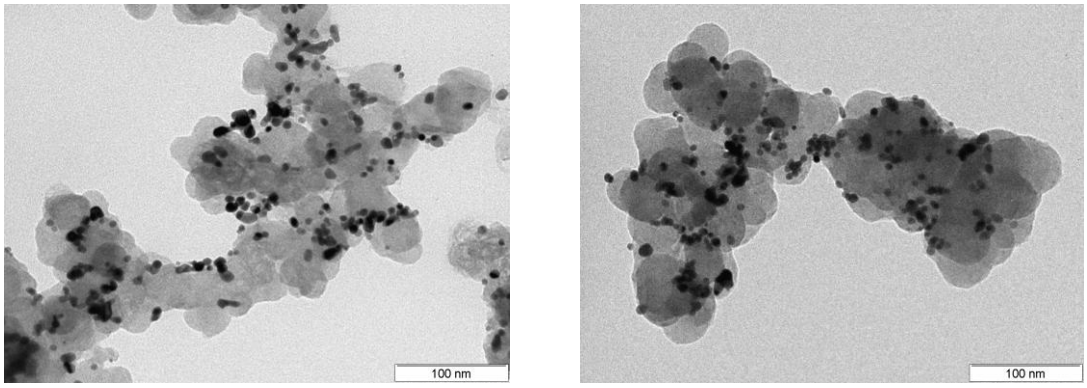

Figure 7. Selected TEM images corresponding to MEA-TEST 1: inlet (left) and outlet (right)

The particle size distributions show a maximum around 5.5-6.0 nm irrespective of the test applied and MEA region analyzed. Table 2 shows the mean particle size for each region analyzed (inlet and outlet).

Table 2. Mean particle size from TEM analysis

MEA	Particle size / nm	
	INLET	OUTLET
MEA-TEST 1	6.0 ± 0.2	5.4 ± 0.1
MEA-TEST 2	5.9 ± 0.1	5.5 ± 0.1
MEA-TEST 3	6.0 ± 0.1	5.2 ± 0.1

9. Modeling of the Electrochemical Interface (FORTH)

Based on experimental observations, it is clear that as the partial pressure of H_2 is reduced, (due to H_2 dilution in Ar or CO poisoning), a third semicircle appears and grows substantially. In literature the appearance of a 3d semicircle at the low frequency range is often attributed to cathode dynamics, more specifically to i) Bounded Warburg Diffusion, due to the transport losses of O_2 in GDL and CL, ii) to oscillations of O_2 concentrations in cathode flow channels, and iii) relaxation and diffusion of oxygenated intermediate species in cathode catalyst layer.

In this task hydrogen adsorption relaxation phenomena and the corresponding effects they have on the performance of the fuel cell were numerically investigated using a dynamic 2-D macro-homogeneous mathematical model without transport limitations where HOR kinetics where incorporated explicitly. The two distinct steps of the kinetic mechanism of hydrogen oxidation reaction, H_2 adsorption (Tafel reaction step, rds) and electro-oxidation, (Volmer reaction step),

introduce an hysteresis to the relaxation of the adsorbed intermediate coverage which in turn is translated in the appearance of a third semicircle in ac impedance spectra.

First the model was validated against the polarization curve of the in-house assembled HT-PEMFC were model predictions were in excellent agreement with the experimental I-V polarization curve but was unable to demonstrate the same accuracy under sinusoidal excitation demonstrating that by fitting polarization curve data isn't enough to discover an accurate and unique estimation of the various kinetic parameters.

In order to replicate the experimental effect of lowered H_2 partial pressure, we conducted several simulations first by varying the hydrogen adsorption constant and then by varying the partial pressure of H_2. It was observed that anode polarization resistance increases due to the reduction of H_2 Partial Pressure and a third semicircle appears dictated by the fact that H_2 coverage oscillates out of phase with respect to potential or current dynamic response. This can be due to the significant difference in the rate of adsorption and the electrochemical rate of consumption of H_2 at the electrochemical interface.

In order to verify that H_2 coverage oscillation causes the appearance of this third semicircle, cathode double layer capacitance was set to zero, in order to allow only the capacitive terms of the anode appear on the spectrum. As depicted in Figure 8, two arcs appear in the AC spectrum. The high frequency arc is attributed to the charge transfer reactions across the interface, while the one at the low frequencies is due to the aforementioned hysteresis phenomena between the H_2 coverage and the current dynamic response. If we set the H_2 coverage constant equal to the steady state value, the low frequency arc vanishes. It is clear that the oscillation of adsorbed hydrogen (coverage) is the cause of the third semicircle and not only it gives rise to an adsorption pseudo capacitance, but at the same time it affects the polarization resistance of the electrode (by letting anode exchange current to oscillate). Thus a careful simulation of the AC impedance spectra can be realized through the development of the physical model, in order to draw valuable information on the electrochemical and chemical process at the electrode.

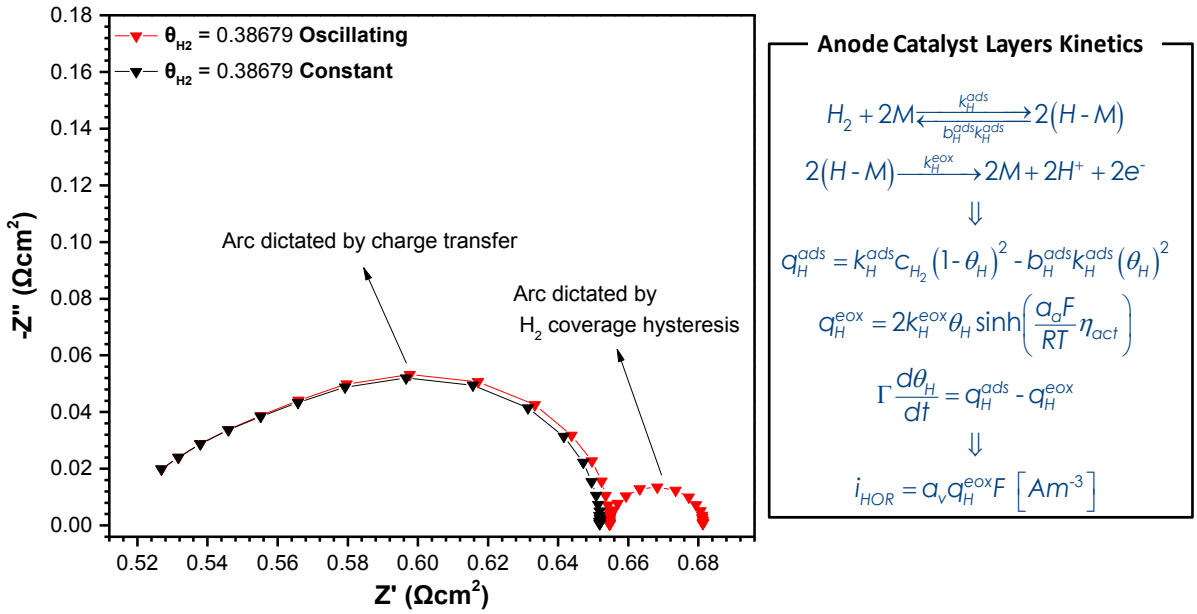

Figure 8. Simulated Impedance Spectra for either oscillating or not coverage, obtained under differential flows (H_2/O_2), current density of 0.2 A/cm^2 at 180^{o}C and the frequency ranged from 50kHz - 0.1mHz.

10. Stack based on metallic bipolar plates (PROTOTECH)

The main objective of this work-package was to optimize individual Fuel Cell components and subsequently produce and test a HT PEM Fuel Cell Stack of 1 kW power output operating on reformate gas within a temperature range of 160-200 °C. Prototech pursued the FC stack concept based on hydroformed thin metal plates. In this concept, each bipolar plate in the stack is formed out of two thin metal plates (0,1 mm thick) welded together so that there is a volume in between, which is used to circulate the cooling liquid. Several different design concepts have been evaluated (square, rectangular or rounded plates; serpentine, interdigated and parallel flowfield channels; internal or external gas manifolding). An analysis of the different design concepts has been performed to investigate the respective advantages and drawbacks. In the end the concept with internal H_2 manifolding and external air/O_2 manifolding using parallel gas distribution channels was chosen. This concept implies that the stack is placed in a thin casing which serves as a part of air manifolding system. A picture of the final thin-metal bipolar plate design is given in Figure 9.

Figure 9. Thin metal bipolar plate design developed by Prototech. H_2- side (l). O_2- side (r).

In parallel to the activities on the bipolar design the selection of materials was driven forward. In order to guarantee the full functionality of the stack despite the challenging material requirements within a HTPEM cell such as low ph-levels, electrical voltages/currents, exposure to acids, gases, moisture and cooling fluid at elevated temperatures of up to 200°C, the materials of the different components needed to be chosen carefully. This includes the sealing material, bipolar-plate base material and bipolar plate coating. For each components suitable material candidates were preselected based on a literature survey and subsequently tested on their suitability for the implementation within a HT PEM FC.

To identify a suitable sealing material Polymer samples were exposed to thermal oil (Galden HT270), concentrated phosphoric acid and temperatures of up to 250°C. Measurements on the elasticity, compression set and swelling were performed at defined time-intervals and used a measure to compare the different samples. IN the end a, a partly fluorinated polymer, Icecube Sealing by Freudenberg Fuel Cell Products, was chosen as the sealing material for Prototechs HT-PEM stack. Despite the initial high hopes for fully fluorinated materials such as Tecnoflon from Solway speciality polymers.

Long-term tests on the different materials for the bipolar plates base material and the coating included the exposure to phosphoric acid and measuring the mass-loss at defined intervals. In addition, conductivity measurements were performed on potential coating materials to evaluate their capability of reducing ohmic losses within the FC. The results finally led to the choice of Inconel 625, which by itself showed an excellent resistance to acidic environments, as a baseline material and a UltraMaxPhase- coating (product by Impact Coatings) for additional corrosion- resistance and reduced ohmic losses. The final hydro-formed bipolar plate produced by Borit from Inconel and coated in UltraMaxPhase is shown in Figure 10.

Figure 10. Final produced HT PEMFC Bipolar Plate.

In addition to the bipolar plates further stack components such as the endplates and the casing were developed and produced in order to gain a fully functional stack assembly. The design of the bipolar plates and the selection of materials was to be validated by assembling a small short-stack to be operated in the respective FC test-stand at Prototechs laboratories. Therefore a stack based on the above described bipolar-plate design and choice of sealing-, base- and coating- materials has been assembled. Steps of the short-stack assembly as well as the final short-stack integrated into the test-environment is shown in Figure 11.

Figure 11. Short-stack assembly and integration

The following short-stack tests focused on the hardware-design verification and at this point not on the electrical performance of the membranes. It was operated at temperatures of 180°C and 190°C while running on pure hydrogen and oxygen gases. The tests achieved good results and the functionality of the sealing-concept-design, cooling-concept-design and the gas-distribution-design could be successfully verified.

The successful short-stack tests subsequently launched the activities on the construction of a 1 kW stack. The key design features are the external oxygen/air manifolding and a thin metal BP construction. This leads to the stack being placed in a thin cylindrical casing, forming the air manifold, and a bit unusual shape. the 1 kW stack is a rather short cylinder with interfaces at the flat end plates. Another important feature is that the design allows for higher operating pressures (up to 10 bar), potentially increasing the power density and efficiency. The model of the Prototech FC stack is shown in Figure 12.

Based on the experience gained from the short-stack assembly described above, a 56-cell stack was to be assembled with the newly developed Advent MEAs in order to achieve the 1kW power target. Since the tolerances of the separate components (plates, sealing, MEAs) are very tight in order the

achieve the mass- and volumetric power-density goals, a very accurate alignment of the sealing and MEAs on the plates and of the plates relative to each other is essential. Slight deviations from the correct postion within the stack can lead to gas- and oil-leaks preventing nominal operation and reaching the power target. Therefore a set of different assembly rigs and tools was developed and manufactured, enabling Prototech to successfully assembly Stacks with multiple cells with the required accuracy. Steps of the assembly process are shown in Figure 13.

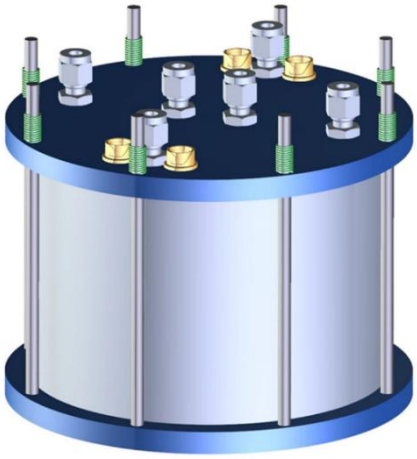

Figure 12. Model of Prototechs developed 1kW HTPEM Stack.

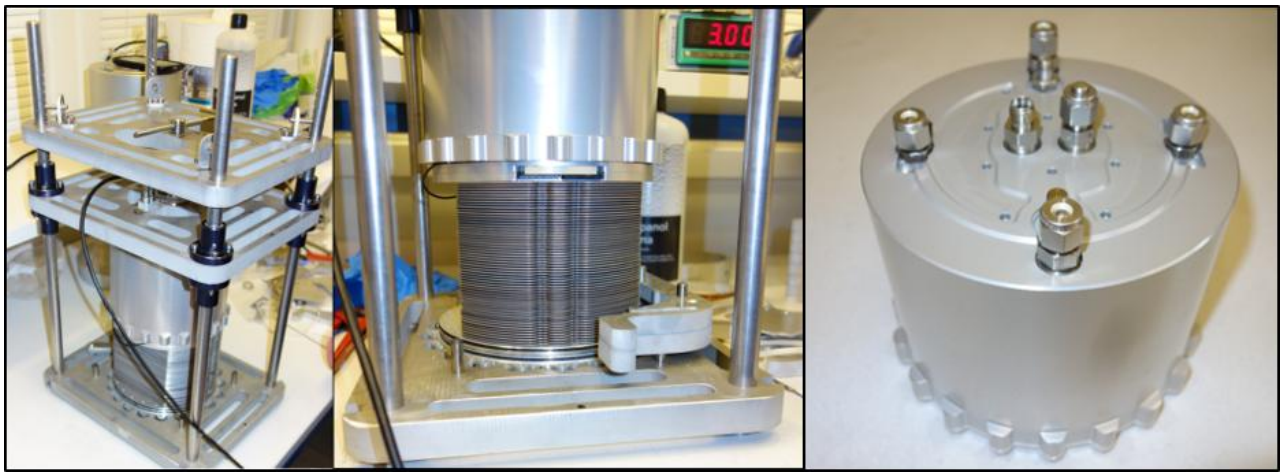

Figure 13. 1kW-stack Assembly

The assembled 1kW stack was subsequently integrated into the test-environment for testing under reformate gas operation. Unlike the stack developed by Advent, it had been decided that the Prototech Stack shall not be coupled to a reformer for testing, but operated under synthetic reformate gas within the Prototech labs.

In order to verify a correct and leak-tight assembly (internal and external), pressure tests have been performed on the fully assembled stacks. The positive results finally demonstrated the suitability of the developed assembly procedure to integrate multiple cell stacks with the necessary accuracy.

The stack was then finally tested at an operational temperature of 185°C at various gas-combinations such as H_2-O_2, H_2-air and reformate-gas/air, successfully demonstrating the suitability of the developed concept for large stack operation.

11. Stack based on graphitic bipolar plates (ADVENT, FORTH)

The second part of the work was oriented on the design and construction of a liquid cooled HT PEMFC stack. First step was the detailed mechanical and thermo-mechanical models for each part separately. Different scenarios have been studied through finite element analysis and after comparing weight, cost, maximum displacement, stress and strain field, safety factor, reduction of complexity & risk for failure, the final list of materials and design was concluded. Special attention was given on the uniform distribution of the compression forces over the MEAs through the specially designed endplates. In regards to the liquid cooling design external heating/cooling plates have been used in order to simplify the construction procedure of the stack and avoid any risks during the operation related to oil leakages and damaging of the MEAs.

Upon design finalization, the HTPEMFC liquid cooled stack of 1kW with graphite resin plates has been successfully manufactured using 43 pieces cross linked Advent TPS MEAs and the operating temperature was 185-200^{o}C. A photo of the constructed stack is given in Figure 14.

Figure 14. The graphite resin based Demstack HT PEMFC stack of 1kW power.

A representative IV curve of the stack with Hydrogen and Air is depicted in Fig.15 and the power output of 1 kW is achieved at 23.5V and 43.8A.

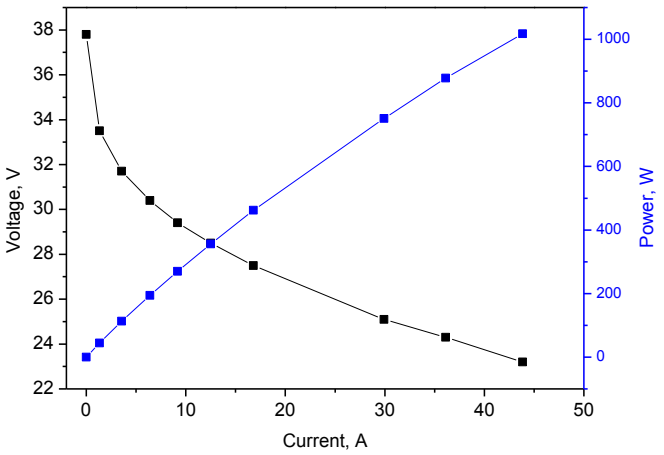

Figure 15. IV curve of 1kW air cooled stack. Temperature: 193^{o}C, Ambient pressure, Feed: H_2 (14lt/min) / Air (67lt/min).

The final step was the successful building and operation of the integrated stack system. In specific, the oil tank, the oil pump able to operate at 180°C, the heat exchanger (air), the silicon based piping system, the control board, thermocouples and a specially designed software (prepared by Helbio) were all connected on a casing as shown in Fig.16. The power of 1kW was achieved with Helbio reformate at 23.5V and 43.8A (operating current density: 0.25A/cm^2). The MEAs showed consistent performance and high stability under successive on off cycles (30 cycles).

Figure 16. Integrated stand alone HTPEMFC stack system of 1kW power.

12. Mathematical modeling of heat distribution in the HT PEMFC stack and experimental validation (UCTP)

A mathematical model was proposed to simulate heat balance and local temperature distribution inside the HT PEM FC stack designed within the DeMstack project. It is characterized by the liquid tempered heat exchanger situated on the two sides of the stack. The mathematical model describes one cell located in the center of the stack, considering this cell as the repeating unit. For this purpose, a macrohomogeneous (or volume-averaged) approach was used. The model is quasi-3-dimensional, or otherwise spatially reduced 2-dimensinal. This means the main in-plane directions (parallel to the membrane plate) are spatially resolved, whereas the third dimension perpendicular to the membrane plane was reduced by means of volume averaged approach. It is possible, because the heat transfer in the perpendicular direction is significantly faster due to short flow path compared to the transport in the in-plane directions. The model consists of stationary heat, charge, mass and material conservation equations. This model was subsequently validated experimentally by temperature profile measured in the bipolar plate of the central cell in the stack at different current loads. The validated model can be used for both bipolar plate and flow-field geometry optimization.

Figure 17 shows typical field of local temperatures in the cell calculated by the mathematical model proposed and implemented. Counter-flow of hydrogen and air are considered in this particular case. As it was found, the uniformity of the current density and temperature is not notably affected neither by (a) the mutual flow direction of hydrogen and air (flow regime) nor (b) value of applied current in the studied range. With respect to (b), temperature profile is predominantly determined by the position of the cooling plates and insulated walls located at the perimeter of the cell. Therefore, highest temperature is observed in the cell center.

Comparison of the experimentally determined and calculated temperature profile is performed in Figure 18 for counter-flow. An excellent agreement was obtained. However, in order to reach this agreement, heat source by dissipation in electric double layer had to be corrected by factor 1.7. This correction of the heat formation is associated with model simplification (spatial reduction of the

model system) neglecting nonuniform current density and overvoltage distribution in the catalyst layer.

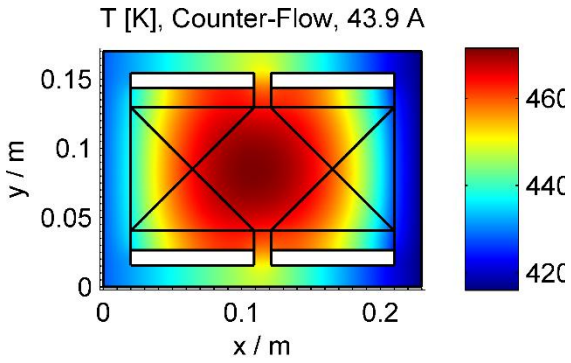

Figure 17. Local field of temperature (T [K]) in single HT PEM FC cell calculated by the validated model for applied current load of 43.8 A and counter-flow regime of the reacting gasses.

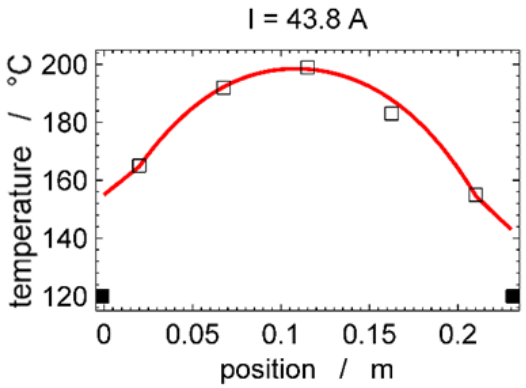

Figure 18. Temperature distribution along the bipolar plate of the central cell in the stack for operating current of 43.8 A, counter-flow regime, solid line – result of the proposed mathematical model, points – experimental data, filled point – temperature of the cooling plate at the air outlet (position = 0 m) and inlet side (position = 0.23 m).

13. Fuel processor and system integration (HELBIO)

The objectives of Helbio were the design and construction of a fuel processor running either on LPG on methane, the development of the control hardware and software and finally the integration of the fuel processor with the high temperature PEM fuel cell derived from WP4. The methodology followed for accomplishing the above tasks are analyzed in the following paragraphs.

Steps followed in brief:

1) Formulation of the Process flow diagram and calculation of the mass and energy balances
2) Piping and instrumentation diagram
3) Mechanical system design and construction (fuel processor)
4) Control hardware design and construction
5) Integration of the fuel processor with the fuel cell

1) Mass and energy balances and process flow diagram (PFD)

Mass and energy balances for each reactor were calculated assuming that the reactor(s) are under thermodynamic equilibrium at pre-selected operating conditions (steam to carbon ratio, temperature, pressure etc.) The parameters were chosen from HELBIO's and based on previous experience in designing similar system. The important figure in order to start the design of the fuel processor, is the quantity of the produced hydrogen; this figure was calculated based on Advent's experimental data of (IV curves) and the projected geometrical characteristics of the fuel cell (number of cells, MEA area etc). The calculated consumption of hydrogen from the fuel cell is 1 Nm3/h and applying a safety factor of 20% the maximum hydrogen production capacity of the fuel processor was set to 1.2 Nm^3/h.

A draft process for the production of a rich to hydrogen gas stream able to feed a high temperature PEM fuel cell is presented in Fig. 19. In specific, the catalytic reactions that take place are the steam reforming along with the water gas shift reaction, resulting in the production of a reformate gas with the following composition: 70-75% H_2, 20-24% CO_2, 0.5-1.5% CO and CH_4<2%.

Based on the above scheme, the detailed mass and energy balances were generated as well as the detailed process flow diagramm of the system.

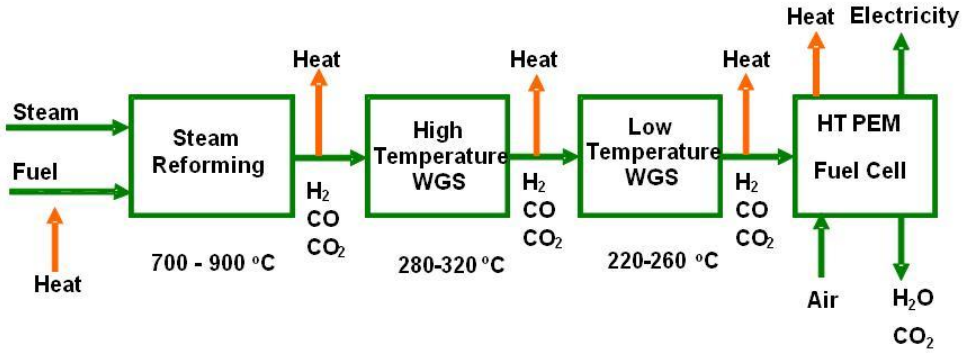

Figure 19. Draft process for energy production route via hydrogen produced by steam reforming process.

The fuel processor consisted of the following parts:

i) Reforming reactor, where the fuel is converted to a mixture of hydrogen and carbon oxides (according to steam reforming reaction).

ii) Water Gas Shift reactor, where the carbon monoxide reacts with steam to produce carbon dioxide and hydrogen.

iii) Steam Generator, where is produced the steam required for steam reforming reaction.

iv) Heat exchangers, to utilize waste heat.

The specifications of the fuel processor defined (based on the requirements and demands of the fuel cell) in the production of a rich to hydrogen (>70% H_2, in dry basis), reformate gas, containing carbon monoxide in concentrations between 0.5 – 3 vol. % (dry).

2) Piping and instrumentation diagram (P&ID) and reactor& heat exchange sizing

Next step in the designing process of the fuel processor, was to draw-up the Piping and Instrumentation Diagram, P&ID. By this process the various peripherals and instruments which are necessary for the safe operation of the system were identified. In particular, based on the mass balances and the PFD, the needs for the water, fuel and air needs were found and the respective specification for each peripheral was set. Further to the above, the necessary instruments for monitoring and adjustment of various parameters (e.g. temperature pressure, flow etc.) were also identified and placed in the appropriate sampling of monitoring position so as to enable a problems-free operation of the system.

The resulted P&ID was used for the preliminary HazOp analysis. In HazOp analysis, each deviation was categorized as Low, Moderate and High, depending of the safety impact (eg. Personnel injuries etc.).

3) Mechanical design and system construction

Equipment sizing (i.e. process reactor and heat exchangers) was conducted based on the thermodynamic properties of each stream, heat exchanger's theory and reactor design, as well as on reactions equilibrium.

The selection of catalytic materials used in the fuel processor was based on previous experience of Helbio and the literature study about relative processes as well.

The catalytic reactions which will take place inside the fuel processor are the following: the steam reforming reaction (endothermic) for the conversion of the fuel to a hydrogen rich stream, the fuel combustion (exothermic) for production of heat which is used in the steam reforming reaction and the water gas shift reaction (exothermic). The two first reactions take place inside the reforming reactor (reformer), while the latter one occurs in the shift reactors placed in series with intermediate cooling steps. The former named as High Temperature Shift reactor and the latter Low Temperature Shift reactor.

The construction of the fuel processor included the following steps:

i) Design and dimensioning of the fuel processor sub-systems
ii) Construction of fuel processor sub-systems,
iii) Testing of fuel processor subsystems.

Testing of the fuel processor

The abovementioned fuel processor was tested using various feeding fuels; in specific with commercial propane and methane, while its performance characteristics were evaluated under various operating conditions. The operating parameters examined were the S/C (steam/carbon) ratio and hydrogen production capacity. In addition the catalytic performance of each reactor was tested under steady state at pre-selected S/C ratio and hydrogen capacity.

The main reactions taking place in a steam methane reformer (SMR) where methane reacts with steam to produce hydrogen and carbon monoxide are as follows:

$$CH_4 + H_2O \rightarrow CO + 3H_2 \quad (1)$$

Simultaneously with the reforming reactions, Water Gas Shift reaction take place in the reformer where CO reacts with H_2O in order to produce CO_2 and H_2:

$$CO + H_2O \rightarrow CO_2 + H_2 \quad (2)$$

Therefore, the reaction products are CO, CO_2, H_2 and CH_4. In case of a propane steam reformer propane reacts with steam (steam reforming) to produce hydrogen and carbon monoxide as follows:

$$C_3H_8 + 3H_2O \rightarrow 3CO + 7H_2 \quad (3)$$

Simultaneously as in the case of methane reforming, the Water Gas Shift reaction takes place as described in Eq. (2). Moreover, a part of the propane doesn't react or it is converted to CH_4. Therefore, the reaction products are CO, CO_2, H_2, CH_4 and C_3H_8. The reformer was tested under selected experimental condition so as to identify its performance characteristics. Fuel employed were CH_4 and commercial propane.

The construction of the fuel processor was completed by the mechanical integration of its various sub-systems (see Fig.21).

4) Control hardware design and construction

The control system (see Fig.20) is based on a microcontroller. The control board consists of the main controller, analog inputs and outputs connection terminals, K-type and Pt100 connection terminals.

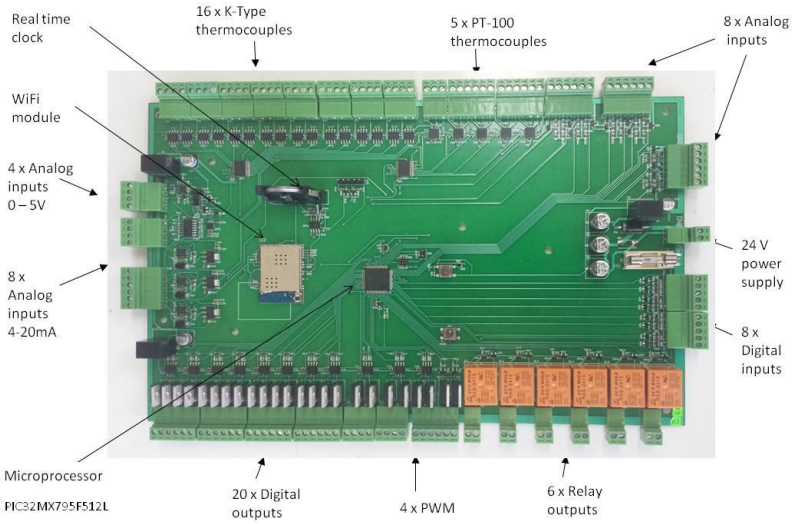

Figure 20. The control system (hardware) assembly.

The electrical devices are driven using NPN transistors or relays while control signals like: 4-20mA, Width Pulse Modulation (PWM) or 0-5V are also available.

The board is equipped with a real time clock for data logging while the HMI is equipped with a SD card slot for data recording and storing. Finally the user can connect to the system using the WiFi capability using a web browser

5) Integration of the fuel processor with the fuel cell and testing of the complete system

The steps followed towards the integration of both subsystems namely the fuel processor and the fuel cell and the final testing of the complete system are described in the following lines:

Assembly of the fuel cell stack with the associate peripherals was accomplished following the piping and instrumentation diagram especially drawn for the fuel cell subsystem. This task was a joint activity between HELBIO and FORTH. The fuel cell subsystem is shown in Fig.21. It consisted of the various peripherals e.g. an oil cooled stack, the air blower and a closed loop oil cooling circuit. In particular, the latter consists of an oil pump equipped with suitable head to sustain its operation at elevated coolant temperatures (e.g. >150^{o}C), the radiator which is used to dissipate the heat generated in the fuel cell stack during its operation. In addition to the above, several thermocouples and pressure transducers are used a) to monitor and adjust the temperatures inside the fuel cell.

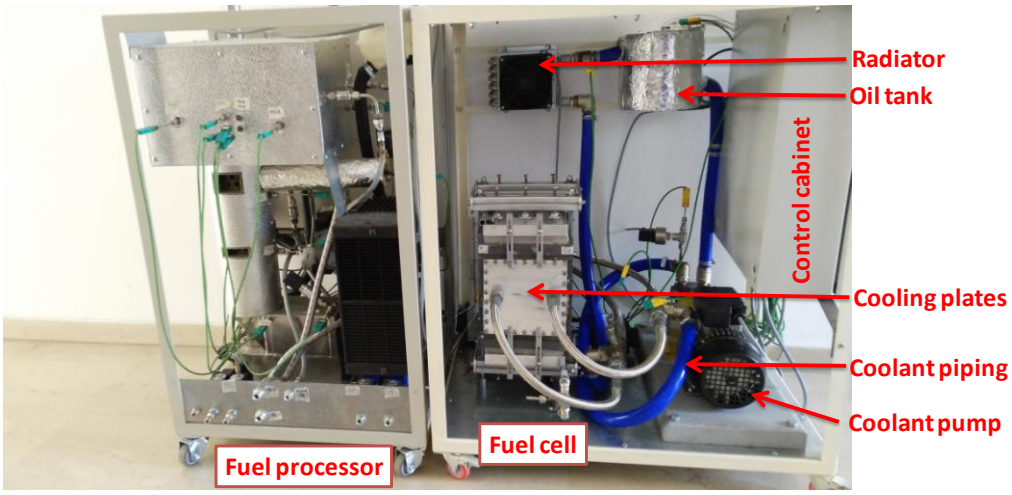

Figure 21. Picture of the fuel cell subsystem assembly and its integration with the fuel cell.

14. Testing of the integrated system (HELBIO, FORTH, ADVENT)

After the integration of the fuel processor and the fuel cell subsystems, the final stage was the testing of the equipment in auto mode using the developed control software for a) software debugging and b) fine tuning of the equipment. Both systems are ready to operate in auto mode for long term testing. Typical results for the testing of the fuel cell subsystem is shown in Fig. 22. During the start up phase the fuel cell stack was initially heated employing the 'hot' coolant oil without hydrogen flow. After the temperature at the middle of the stack exceeded 100 ^{o}C, reformate hydrogen was fed to the stack. At the same time a variable load was applied. The heating up process was then continued maintaining the stack voltage between 22 to 23V until the temperature at the middle of the stack was ~200 ^{o}C. After the desired temperature was reached, the system was left to equilibrate for 10 minutes at a preselected operating current and the cell voltages were recorded. In general the fuel cell stack system appears to be very flexible in delivering in a sustainable way 500W-1000W with fast dynamic response. This is due to the high tolerance of the MEAs to operate without degradation within the temperature range of 160-200^{o}C.

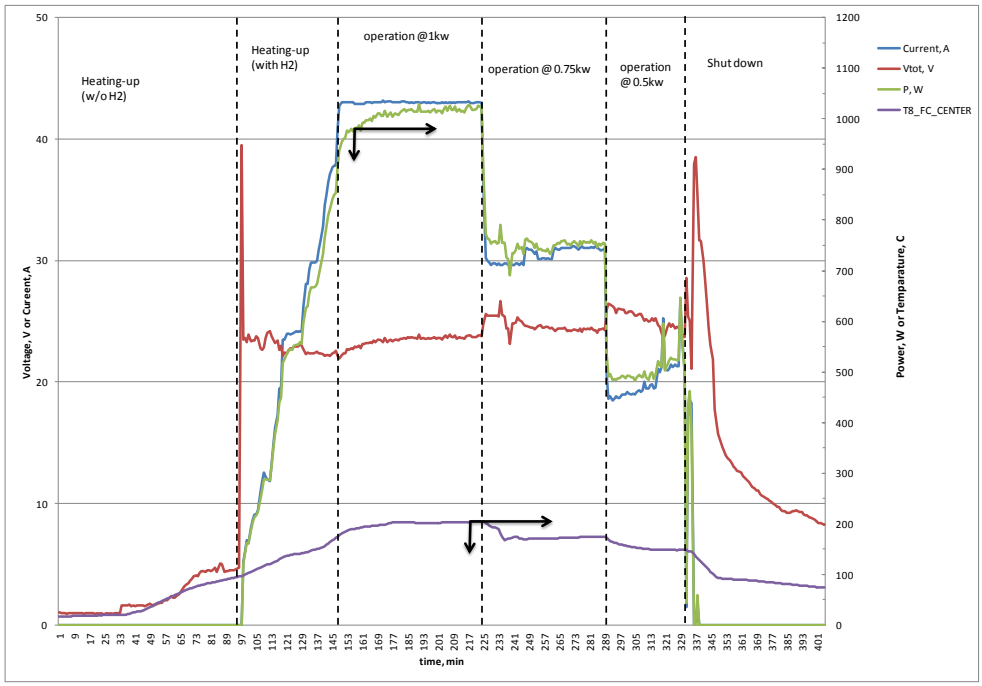

Figure 22. Fuel cell operation consisting of: the heating-up phase, the operation of the fuel cell system at the selected operating capacities with reformate hydrogen and the shutdown phase.

In conclusion:

- The fuel processor design and construction were completed. The fuel processor was tested and its performance characteristics were within the specification set.
- Integration of the fuel processor and the fuel cell was completed successful. Operation of the completed system was conducted successfully.
- The fuel cell stack system appears to be very flexible in delivering in a sustainable way 500W-1000W with fast dynamic response.
- Performance of the fuel cell goes through a maximum as the water content increases in the gas phase (e.g. dew point of 40 ^{o}C)
- Start-stop cycling of the fuel cell with the fuel processor showed no decrease in the performance of the fuel cell.

Experiments will continue after the end of DeMStack, as the partners involved in this task have strong interest towards the development of similar products incorporating high temperature PEM fuel cell and reformer.

Description of the potential impact, the main dissemination activities and the exploitation of results

The impact of the project on the scientific technological and economic development capacity of the participating and industrial partners is significant, not only during the project's execution but in a longer term. DeMStack resulted in a robust and highly efficient HT PEMFC stack with validated stable performance. The academic partners offered the scientific tools through materials development and mathematical modeling as a diagnostic and design tool for the optimization of the MEA's performance, as well as assisted on the advanced design of the fuel cell stack. The three industrial partners of the consortium contributed with more applied research toward the development of components, subsystems and the efficient system integration. Great knowledge and interface was generated that promotes the work of the research institutions involved and has significant impact on the future evolution of their research activities. The first level of results exploitation is in the form of 7 peer-reviewed publications and conference presentations. More specifically, 38 papers containing results of the DeMStack project were communicated to the scientific and broader audience though the participation of the consortium to different events: 18 oral and 19 poster presentations to conferences, 1 interview and 2 oral presentation to the FCHJU PRD took place, and the consortium attended 25 different events. Moreover, FORTH organized the 3degis conference, the 3rd International Workshop on Degradation Issues of Fuel Cells and Electrolysers, which was held in Santorini, Greece on September 29th to October 1st, 2015. The workshop comprised sessions on the state of the art reviews on degradation issues of fuel cells, such as Polymer Electrolyte Fuel Cell (PEFC) and Solid Oxide Fuel Cell (SOFC) and in electrolysis mode (PEMWEC and SOEC). A panel discussion session took place, suggesting future directions in fuel cell degradation research. A domain was created at the beginning of the project: demstack.iceht.forth.gr. The user-friendly website contains a general description of the project, description of the consortium, a news area (including important dates, a regularly updated list of publications etc) and contact details. For public communication purposes, non-sensitive information was shared on this public web site.

More importantly, the three SMEs involved have already ensured the fast exploitation of the results through the optimization of their commercial products and improvements in their technology. For Advent and Prototech, this was their first collaboration and the first HT PEMFC stack they developed with the specific characteristics. Important experience and knowledge exchange took place and their level of experience advanced, which can broaden their cooperation with industrial end-users. Advent is mainly a manufacturer of Membrane Electrode Assemblies (MEAs), while during the past few years they are trying to integrate their product into a HT FC stack. Through DeMStack, they have broaden their activities resulting into a reliable prototype to demonstrate to potential buyers and future development partners. Prototech has fuel cells and hydrogen technologies as one of its main market areas, while has a patent on an integrated reformer-burner for HT PEMFC stacks. Based on the project, Prototech plans to further develop APUs (auxiliary power units) using this technology.

DeMStack was also the initiation of more intense joint activities between Advent and Helbio, since the first fuel cell/fuel processor prototype based on their technology was constructed within this project (a low-cost HT PEMFC 1 kW stack based on Advent PEM and constructed from the DeMStack optimized components is integrated with a fuel processor specifically built to suit the demands of the FC stack). The robustness of the stack, the simplicity of BoP, the operational stability and the user friendly operation of the integrated system into a commercially reliable product were demonstrated and is expected to help the penetration of such technologies into the market. The benchmarking especially of the graphitic stack to similar technology market products appears to be more advanced in terms of the aforementioned characteristics. Being able to demonstrate the efficient

operation of the prototype, the companies can jointly pursue further funding (field testing) and open a new path in the hydrogen market.

Based on the advances within DeMStack, the partners have teamed up to pursue common goals and end-users, while will try to participate in new proposal submissions with higher TRL for the continuation and substantiation of their cooperation in the FC market. Moreover, European Space Agency has already signed separate contracts with FORTH, ADVENT and Prototech to manufacture systems based on the HT PEM technology for space applications in telecom satellites.

The aforementioned actions clearly demonstrate the multilevel commercialization possibilities of the DeMStack prototype. DeMStack is a first attempt to combine optimized components and methodologies into an integrated system. Possible applications of this technology can be found in Auxiliary power units (3-10kW), CHP units, Battery chargers with LPG (300 W), Power supply in remote/off grid areas (2kW), Regenerative fuel cells for space (3kW satellites) and Stationary back up power systems. Further RTD is certainly necessary to complete the transition of small scale to large scale level, and to determine the optimized operation conditions and stability of the system (including slight modifications to components according to findings). Nevertheless, the successful implementation of the DeMStack product into the hydrogen existing and future infrastructure will open new perspectives in fuel cell technology, a fact that will contribute to the objectives of the European Platform to gain world leadership and offer substantial scientific, economic, energy and environmental benefits. The social impact of the proposed technology, the use of fuel cells and the resulted product in terms of energy aspects and environmental quality is obvious. The high quality energy produced by a fuel cell, zero emissions of pollutants and greenhouse gases and the possibility to improve the living conditions and infrastructures in less favored regions are only part of the benefits. Moreover, the economic impact is noteworthy, besides the potential of this technology to ensure a more secure, strong and growing European economy. In the short-term, DeMStack attracted and employed young scientists with advanced knowledge, while generated highly-skilled scientists and researchers. The established contact between academia and industry can stimulate high level scientific career opportunities. As described above, the present project significantly contributed to the sustainable growth of the participants with the corresponding impact in employment.